

## Article

# Facile Electrochemical Biosensing Platform Based on Laser Induced Graphene/Laccase Electrode for the Effective Determination of Gallic Acid

Xi Lin <sup>1</sup>, Yuchen Zhou <sup>1,2</sup>, Zhenfeng Lei <sup>1</sup>, Rui Chen <sup>1</sup>, Wanchun Chen <sup>1</sup>, Xiangying Meng <sup>3,\*</sup>  and Yanxia Li <sup>1,4,\*</sup> <sup>1</sup> College of Materials and Chemical Engineering, Minjiang University, Fuzhou 350108, China<sup>2</sup> College of Chemistry and Materials Science, Fujian Normal University, Fuzhou 350108, China<sup>3</sup> School of Medical Laboratory, Weifang Medical University, Weifang 261053, China<sup>4</sup> Fujian Engineering and Research Center of New Chinese Lacquer Materials, Fuzhou 350108, China

\* Correspondence: mengxy2015@wfmuc.edu.cn (X.M.); yxli09@163.com (Y.L.)

**Abstract:** In this study, a facile electrochemical biosensing platform was fabricated with Laccase (Lac) immobilized on laser-induced graphene (LIG) electrode by glutaraldehyde covalently binding for the effective determination of gallic acid (GA). The patterned graphene for the LIG electrode was prepared by a one-step laser direct writing on the polyimide film in ambient air. The sheet layer and spatial mesh structures of LIG give the prepared LIG electrode a large specific surface area and good conductivity. The oxygen enrichment and good hydrophilicity cause LIG to favor covalent crosslinking with laccase through glutaraldehyde. The electrochemical sensor of GA on the prepared electrode was determined by chronoamperometry. Results show that the current signals of the laccase electrodes had an excellent linear relationship with GA in the concentration range of 0.1–20 mmol/L with a detection limit of 0.07 mmol/L under optimized experimental conditions. The prepared GA sensor with good selectivity, regeneration, and stability can be applied to biological samples such as sweat, urine and serum without needing sample pretreatment.

**Keywords:** laser induced graphene; laccase; gallic acid; electrochemical biosensor



**Citation:** Lin, X.; Zhou, Y.; Lei, Z.; Chen, R.; Chen, W.; Meng, X.; Li, Y. Facile Electrochemical Biosensing Platform Based on Laser Induced Graphene/Laccase Electrode for the Effective Determination of Gallic Acid. *Processes* **2023**, *11*, 2048. <https://doi.org/10.3390/pr11072048>

Academic Editors: Lei Shi and Haiyong Zhang

Received: 16 June 2023

Revised: 5 July 2023

Accepted: 7 July 2023

Published: 9 July 2023



**Copyright:** © 2023 by the authors. Licensee MDPI, Basel, Switzerland. This article is an open access article distributed under the terms and conditions of the Creative Commons Attribution (CC BY) license (<https://creativecommons.org/licenses/by/4.0/>).

## 1. Introduction

The electrochemical biosensor is a sensor device that combines the characteristics of electrochemical sensing and biomolecular specific recognition [1,2]. Due to the high sensitivity and selectivity, quick response, and easy signal detection, electrochemical biosensors play a crucial role in laboratory and clinical practice, which can analyze various chemical and biological objectives, such as applying them to cancer biomarker determination for early diagnosis of cancer and providing higher diagnostic accuracy [3,4]. Generally speaking, the ultimate goal of electrochemical sensors is to build a more simple, sensitive, and reliable sensing platform for further amplifying the detection signal and improving the accuracy. The development of new functional nano materials and nanotechnology provides new possibilities to improve the performance of electrochemical sensors [5,6]. Hence, finding high-performance electrode materials is always one of the critical points in preparing excellent electrochemical sensors. Graphene has caused a tremendous research upsurge due to its particular electricity, heat, mechanics, and other properties. Since the discovery of graphene, various techniques, including micromechanical exfoliation, chemical vapor deposition, epitaxial growth, and chemical reduction in graphite oxide for graphene preparation, have been constantly explored to supply the demand for its different practical applications. Laser has the characteristics of directional luminescence, high energy density, and high brightness, which provides a new research direction for thin film preparation [7]. More importantly, the application of lasers in experiments usually does not change the principle of the experiment; it only changes the heating mode, which significantly shortens

the reaction time and improves the experimental efficiency. Graphene synthesis methods have been studied around the large area of preparation and quality improvement. However, for the application in microelectronic equipment, high-performance electronic devices, and sensors, it is more important that the preparation methods of direct preparation, patterning and high efficiency are necessary, which can be easily realized by laser processing [8]. For example, the patterning of graphene can be easily completed by laser movement without complex processing and an additive approach [9]. Moreover, the polyimide precursor and effective laser processing show the great promise of roll-to-roll production. Today, the accurate adjustment of laser energy intensity, direct growth, and rapid manufacturing of graphene allow laser induced graphene (LIG) technology to be widely applied in electronic devices [10], supercapacitors, biosensor [11,12], etc. As a promising uniform multilayer stacked graphene electrode with high porosity and large surface area, the application of LIG electrodes in electrochemical biosensors is just getting underway. Santos et al. reported an IR and UV LIG for dopamine electrochemical sensor. Despite providing lower sensitivity, UV LIG is still an excellent material for DA biosensors, with the advantage of miniaturization [13]. A Diagnostic on a chip platform based on LIG electrochemical biosensor for the detection of SARS-CoV-2 antibodies was applied to assess the vaccinal immune response of the population [14]. More LIG-based electrochemical biosensors with high performance need to be further exploited.

Gallic acid (3,4,5-trihydroxy benzoic acid) (GA), which is a naturally occurring phenolic component, has a strong antioxidant and excellent biological properties, including anti-inflammatory, antihistaminic and antitumor activities, scavenging of free radicals, and protection against cardiovascular diseases [15]. Given that the development of sensitive and selective detection methods for GA biological analysis can help the diagnosis of its related diseases [16], various approaches have been developed to detect GA. Currently, the methods for determining GA mainly include ultraviolet-visible spectroscopy [17], high-performance liquid chromatography [18], flow injection analysis [19], thin layer chromatography [20], and electrochemical methods. Among them, electrochemical sensors have led to considerable interest in detecting biomolecules due to their excellent performance features, such as high sensitivity and selectivity, rapid, cost-effective, miniaturization, portability, and so forth [21–23]. Even so, strategies to reduce the cost, simplify the operation process, and improve the reliable determination of body fluids for GA sensors are still a great challenge.

Laccase is one of the main components of natural lacquer, with a content of about 10%. It exists in the nitrogen-containing substances of natural lacquer, commonly known as lacquer protein and oxidase. It is an indispensable natural organic catalyst for natural paint drying at room temperature. The universality, refractory and toxicity of substrates in nature, and the environmental friendliness of laccase reactions allow laccase to have great application prospects in chemical engineering. At present, the application principle of laccase is to utilize the redox properties of laccase to oxidize toxic aromatic compounds. Laccase has been widely used in industries such as pulp and paper making, sewage treatment, food, organic synthesis, etc. In addition, there are corresponding research reports on laccase in environmental remediation [24], clothing industry [25], drug determination [26], and biosensors [27].

As a typical poly copper oxidase, laccase can catalyze the oxidation of polyphenols and diamines, which has been widely studied in biological determination [28–32]. In this work, the LIG/lac electrode-based electrochemical biosensor with superior performance was prepared for the determination of GA. Patterned micro graphene electrode based on laser direct writing technology was designed with a large specific surface area, good conductivity, and biocompatibility. As a bio-recognition element for the specific response to GA, the active laccase was immobilized on the LIG electrode surface through covalent crosslinking of glutaraldehyde. From the experimental results, the prepared GA sensor showed good performance with low cost, stable performance, and simple operation. Moreover, excellent selectivity makes the sensor successfully applied in complex biological samples, which is

concluded to hold great promise for biological applications. Therefore, this study not only enriches the foundation study about the LIG-based electrochemical biosensors, but also provides an alternative determination method for GA assay.

## 2. Materials and Methods

### 2.1. Materials

The polyimide (PI) sheet (80  $\mu\text{m}$  thickness) was purchased from Tianjin Jiayin Nano Technology Co., Ltd., Tianjin, China. Laccase ( $\geq 0.5$  units/mg) was provided by J&K chemicals reagent Co., Ltd., Beijing, China. Gallic acid (AR,  $\geq 99\%$ ) was provided by Aladdin chemicals reagent Co., Ltd. China. Fetal bovine serum (FBS), phosphate buffered saline (PBS, 0.1 M, pH 4.0), glucose, galactose, lactobionic acid, and arginine of analytical grade and glutaraldehyde (50%) were received from Beijing Dingguo Biotechnology Co., Ltd. (Beijing, China). Artificial urine and artificial sweat were purchased from Shanghai Yuanye Biotechnology Co., Ltd. A conductive silver paint pen was purchased from Shenzhen Osborne Co., Ltd., Shenzhen, China, and silver/silver chloride paste was purchased from Guangzhou Yinbiao Trading Co., Ltd. China. Milli-Q purified water (Millipore, St. Louis, MO, USA) was used for all experiments throughout this study.

### 2.2. Fabrication of LIG Electrode

The LIG electrode was manufactured in our laboratory. The preparation of LIG electrodes was performed according to our previous research [33]. Briefly, a fully integrated LIG electrode was fabricated by 450 nm laser irradiation over a PI sheet. Continuous semiconductor laser was used in the preparation of LIG (Nano Pro-III, Tianjin Jiayin Nano Technology Co., Ltd., Tianjin, China, voltage 5 V, laser intensity: 60%, carving depth: 15%). The three-electrode patterns were designed by drawing through PowerPoint. The classical three-electrode system consisted of a LIG electrode (3 mm diameter) as the working electrode (WE), a hand-coated Ag/AgCl paste as the reference electrode (RE), and graphene as the counter electrode (CE). The end of the three electrodes was hand-coated with a conductive silver paste, to ensure better electrical contact with the electrochemical workstation. The work area was defined by hydrophobic polydimethylsiloxane (PDMS). In brief, a calculated amount of PDMS and the curing agent (10:1 ratio) were mixed properly and precured at 85  $^{\circ}\text{C}$  for 5 min. Thereafter, a small amount of PDMS semi curing solution was applied with a needle tip to the tangent line of the working electrode circle to fix the area of the work area.

### 2.3. Fabrication of LIG/Lac Electrode

A volume of 20  $\mu\text{L}$  mixed solution of 3% glutaraldehyde and 5 mg/mL laccase containing 1% bovine serum albumin (BSA) with a ratio of 1:1 was dropped directly on LIG work area. After incubation for 30 min, the modified electrodes (LIG/Lac electrode) were cleaned with ultrapure water, dried at room temperature, and then stored at 4  $^{\circ}\text{C}$ .

### 2.4. Electrochemical Analysis

The electrochemical measurements were performed with a Mini electrochemical analyzer (Sensit BT, PalmSens, Houten, The Netherlands) controlled by a PC running PStTrace software version 5.8 at room temperature. A solution of 50  $\mu\text{L}$  5 mM  $\text{K}_3[\text{Fe}(\text{CN})_6]$  containing 0.1 M KCl was dropped on the LIG/Lac electrode for cyclic voltammetry (CV) scanning in the potential region of  $-0.3$  V and 0.4 V at a scan rate of  $0.1 \text{ V}\cdot\text{s}^{-1}$ . Chronoamperometric analysis of LIG/Lac electrode for GA sensor was performed with working potential at 0.4 V in 10 mM PBS (pH 4.0). 50  $\mu\text{L}$  sample solution was dropped on the LIG/Lac electrode for complete coverage of three electrodes. Before each measurement, homogeneously mixing is necessary, and the initial current signals also need to be recorded.

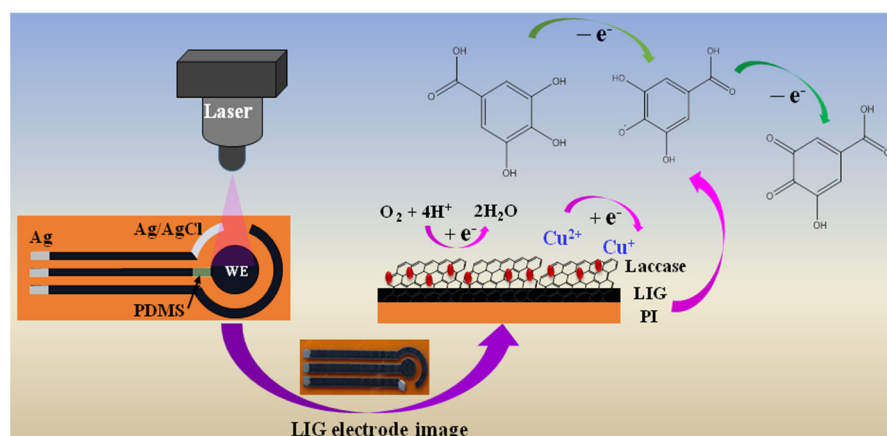
### 2.5. Characterization

The surface morphologies of the prepared LIG electrodes were characterized by scanning electron microscope (SEM, SU8000, Hitachi, Japan). The morphologies and structures of the LIG nanomaterials were examined by transmission electron microscope (TEM, Tecnai F30 G<sup>2</sup> STWIN 300 kV, Hillsboro, OR, USA). Elemental analysis of C, N, and O was performed with energy dispersive X-ray spectroscopy (EDS, EDAX TEAM<sup>TM</sup>, DE, USA). Raman spectroscopy was performed using a Thermo Scientific DXR2 microscope (Waltham, MA, USA). Powder X-ray diffraction (XRD) patterns were made with an X-ray diffractometer (Rigku SmartLab, Tokyo, Japan) using Cu-K $\alpha$  radiation. Thermogravimetric analysis (TGA, STA 449C Netzsch, Selb, Germany) was used to characterize the assembly effect of laccase on LIG. The LIG nanomaterials were scraped off from the work area of the LIG and LIG/Lac electrodes for TEM, XRD, Raman spectroscopy, and TGA characterization.

## 3. Results and Discussion

### 3.1. LIG/Lac-Based GA Sensor

The strategy of the GA sensor based on LIG/Lac electrode shows in Scheme 1. Firstly, the classical three-electrode system of LIG electrodes was prepared using single-step direct laser writing from commercial PI film. The portable and cheap laser can easily realize the graphitization of PI film surface with 450 nm. The whole preparation process is green and environmentally friendly without any chemical reagent. Under optimized lasing conditions, the LIG electrode was produced, ensuring structural integrity on the PI substrate and excellent conductivity and stability. Then, laccase was covalently crosslinked to the surface of WE based on LIG's excellent hydrophilicity and high oxygen content. The excellent hydrophilicity and high oxygen content of LIG was beneficial for the glutaraldehyde-mediated covalent immobilization of laccase on the surface of LIG electrode to construct an amperometric enzyme biosensor for GA. The immobilization of the enzymes on the electrode surfaces is an important step in the preparation of the biosensor, as it preserves the enzymatic activity and designs efficient pathways for electron transfer between the immobilized enzyme and the electrode surface [34]. The direct cross-linking of laccase makes the electrode modification process very convenient, indicating that the LIG/Lac-based GA sensor possess a highly valuable application.



**Scheme 1.** Structure of the LIG electrode and the electrocatalytic action of laccase.

### 3.2. Characterization of LIG

The SEM was used to represent the micromorphology of LIG electrode. As shown in Figure 1A, the SEM image of the LIG electrode reveals a spatial mesh structure with a large specific surface area and adhesion to each other, which are the inherent characteristic of the graphene electrode with good electrical conductivity. The TEM was used to characterize the microstructural information of the prepared LIG. As can be seen from Figure 1B, the sheet layer structure and a large number of folds were on the surface of LIG, which can

increase the specific surface area of the LIG-based electrode. Then, the EDS was used to determine the chemical composition of the LIG. As shown in Figure 1C,D, the content of C, N, and O elements were 96%, 1%, and 3%, respectively. Although the remaining oxygen components of LIG always decrease its conductivity, likely weakening the signal strength of graphene biosensor, they improve its hydrophilicity and provide active sites for functionalization [11], which is a benefit for covalent crosslinking with laccase through glutaraldehyde. The water contact angle test demonstrated that the LIG exhibited good hydrophilicity with a contact angle of  $76.8^\circ$  (Figure 1E). The contact angle increased to  $128.5^\circ$  (Figure 1F), indicating that the hydrophilicity of the LIG/Lac surfaces was decreased with the Lac modification. This phenomenon can be ascribed to the low water solubility of laccase. The results also proved that laccase was successfully modified to the LIG electrode surface.

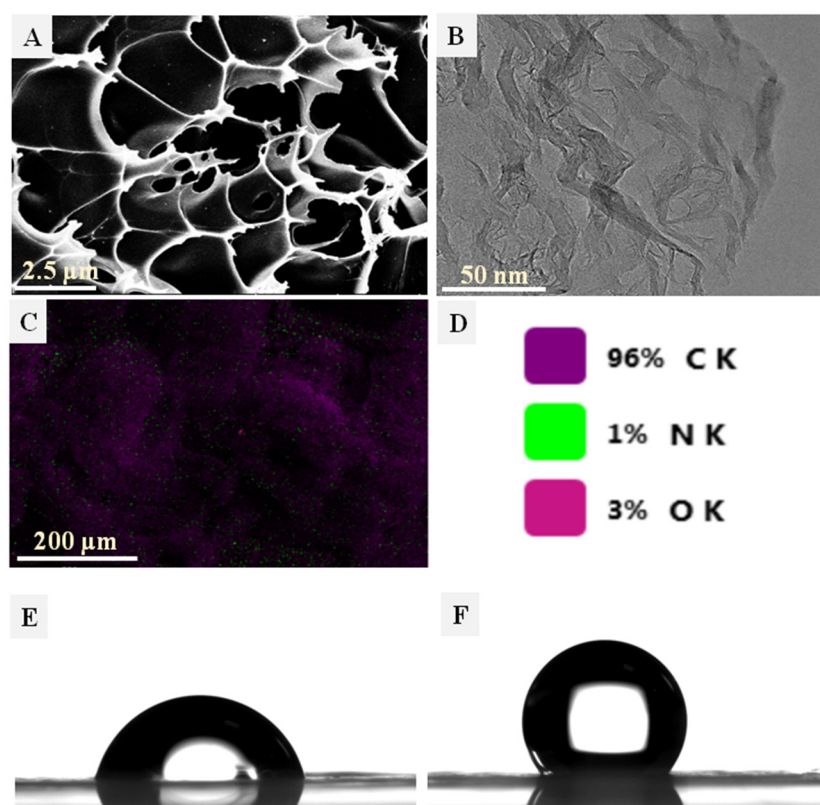


**Figure 1.** Characterizations of LIG. (A) SEM; (B) TEM; (C) EDS images; (D) the content of C, N, and O elements of LIG; and images of contact angle tests of (E) LIG-based electrode; (F) LIG/Lac electrode.

Raman spectra further investigated the formation of the graphitic structure of the LIG. Three typical features of graphene appeared on the spectra as shown in Figure 2A. The D peak at  $1333\text{ cm}^{-1}$  suggested a significant number of  $\text{sp}^3$  centers in the LIG due to structural edge defects and oxygen-containing groups [12]. The G-band at  $1570\text{ cm}^{-1}$  was induced by an  $\text{E}_{2g}$  mode of graphite associated with the stretching motion of  $\text{sp}^2$  carbon atoms, and the 2D band at  $2665\text{ cm}^{-1}$  was originated from the second order of zone-boundary phonons [35]. The shift G and 2D peaks and the wide 2D band suggested that the LIG contained only a few layers of graphene [36]. The ratio  $I_{2D}/I_G$  calculated from Figure 2A was less than 1, indicating the formation of multilayer graphene on the LIG [37]. Figure 2B shows the XRD patterns of the LIG. The typical (002) peak at  $25.9^\circ$  corresponding to d-spacing of  $\sim 0.34\text{ nm}$  [38], and the peak at  $43.2^\circ$  associated with the (100) graphitic crystal phase demonstrated the presence of graphitic structure on the LIG.

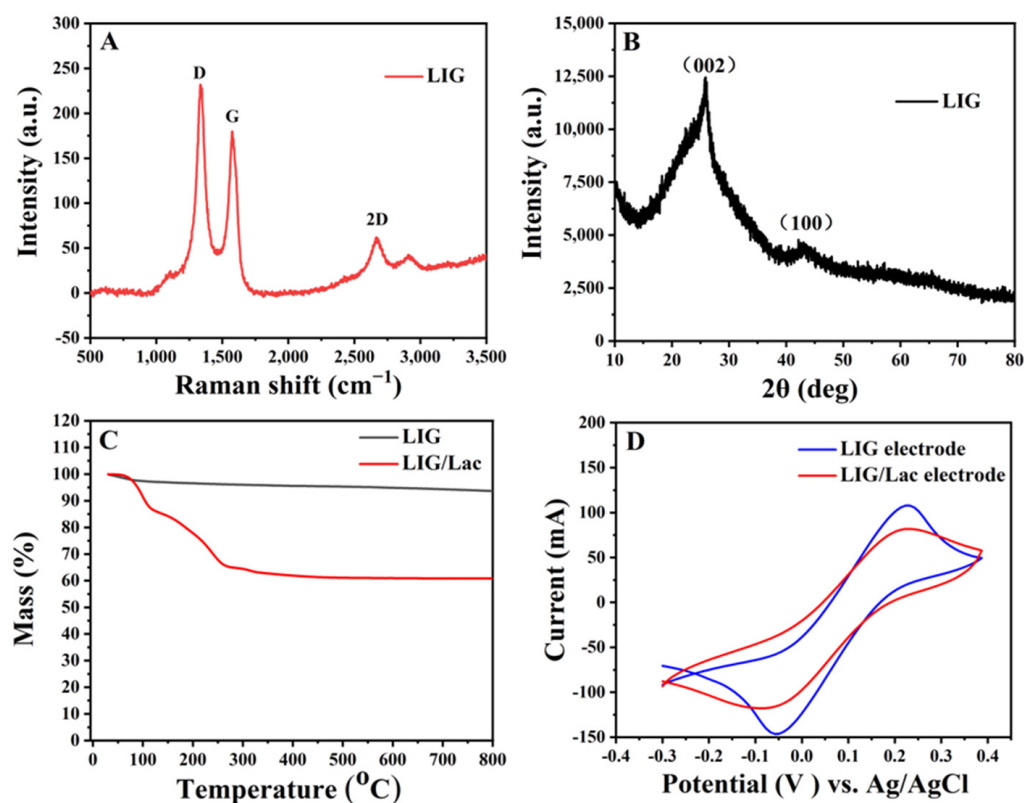


**Figure 2.** Characterizations of LIG. (A) Raman, (B) XRD of LIG, (C) TG analysis of LIG and LIG/Lac nanomaterials, (D) Electrochemical analysis of LIG and LIG/Lac electrodes in 5 mmol/L  $\text{K}_3[\text{Fe}(\text{CN})_6]$  containing 0.1 M KCl, scan rate:  $0.1 \text{ V}\cdot\text{s}^{-1}$ .

TGA can be effectively used for measuring a material's weight loss at particular temperatures. The TGA curves of LIG and LIG/Lac nanocomposites scraped off from the surface of LIG, and LIG/Lac electrodes were presented in the temperature range from  $\sim 30^\circ\text{C}$  up to  $800^\circ\text{C}$ . As shown in Figure 2C, the weight loss rate of LIG nanomaterials was  $\sim 8\%$ . That was mainly because the O and N contained in the LIG materials were removed under high temperature except for about 3% moisture, which was approximately in agreement with the result of the EDS analysis. In addition, the weight loss rate of LIG/Lac nanomaterials was  $\sim 40\%$ , which was obviously higher than the bare LIG, can be mainly attributed to the loss of laccase in the nanocomposites and also indicated that laccase has been successfully modified onto the LIG electrode.

The electrochemical performance of the prepared LIG and LIG/Lac electrodes were thoroughly investigated in order to verify the effect of laccase modification on the modified electrodes. The electrochemical activity of LIG and LIG/Lac electrodes in  $\text{K}_3[\text{Fe}(\text{CN})_6]$  solution was carried out by CV. Figure 2D revealed that the LIG electrode showed excellent electrochemical activity with a pair of the reversible curve and redox peaks, primarily due to the mesoporous honeycomb structure and good conductivity of the prepared LIG. After being modified with laccase, the redox peak current produced by LIG/Lac electrode decreased compared to the LIG electrode, indicating that laccase, as an electrically inert biomacromolecule, was successfully assembled on the LIG electrode surface. Nevertheless, the LIG/Lac electrode exhibited well-defined quasi-reversible redox. The result demonstrated that the LIG/Lac electrode still has good electrochemical activity, which was conducive to GA sensing.

### 3.3. Optimization of Laccase Dosage

The laccase dosage was investigated to ensure that the laccase was thoroughly and effectively immobilized on the electrode surface. Laccase with different concentrations was

immobilized on the electrode surface by glutaraldehyde. The current signals were obtained by chronoamperometric analysis on the LIG/Lac electrode for the GA sensor. As seen in Figure 3, the currents increased gradually with the increase in laccase concentration. This phenomenon demonstrated that the assembly of laccase increased the current signal of the prepared sensor to GA, since the immobilized laccase have reached saturation when the laccase concentration increased to 2.0 mg/mL. Therefore, 2.0 mg/mL was selected as the optimized concentration of laccase in the experiment.

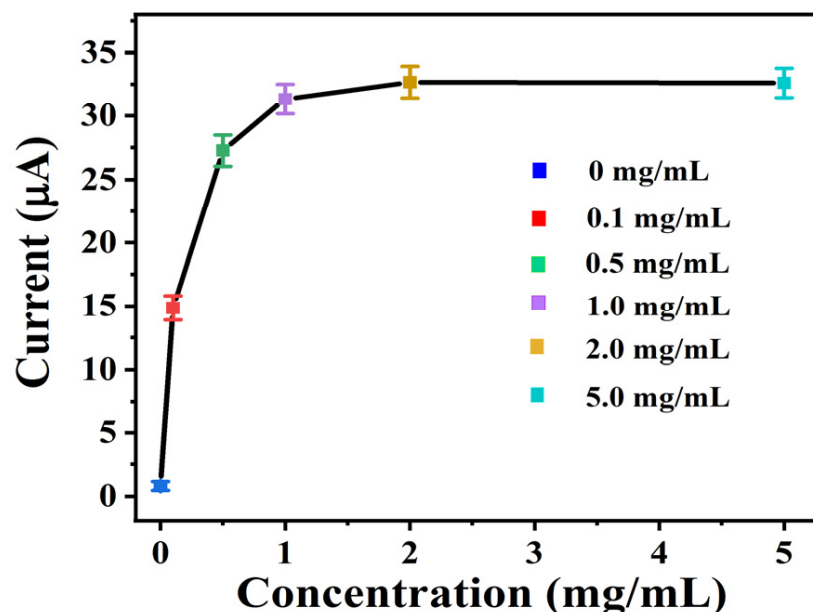


**Figure 3.** Curve of currents changed with laccase dosage. Applied potential is 0.4 V vs. Ag/AgCl. 10 mmol/L PBS at pH 4.0. GA concentration: 5.0 mmol/L.

### 3.4. Chronoamperometry Determination

The Chronoamperometric analysis of the LIG and LIG/Lac electrodes was tested towards different GA concentrations. To perform the amperometric measurements, 50 µL of 10 mmol/L PBS (pH 4.0) were dropped on the surface of LIG and LIG/Lac electrodes for complete coverage of three electrodes. Increasing concentrations of GA were incrementally added on the same electrode in the range from 0.1 to 20 mmol/L, and the current signals were recorded every 60 s.

As shown in Figure 4, the *i*-*t* current signals based on the LIG and LIG/Lac electrodes increased with the increase in GA concentration by applying a constant potential at 0.4 V (Figure 4A) and 0.5 V (Figure 4C), respectively. Figure 4B (0.4 V) and Figure 4D (0.5 V) show that the recorded current signals increased linearly with the GA concentration range from 0.1 to 20 mmol/L. It is easy to see that both LIG and LIG/Lac electrodes realized effective GA sensing with good linearity and sensitivity. However, the LIG/Lac electrode demonstrated a better current response to GA than the LIG electrode, indicating that the determination sensitivity was effectively improved by the assembly of laccase on the LIG electrode. Compared with the LIG electrode, although the laccase modified electrode hindered the electron transfer on the electrode surface (Figure 2D), it showed a sensitive chronoamperometric response to GA, which proved that laccase had excellent catalytic activity to GA (Figure 4B,D). The better determination sensitivity for the LIG/Lac electrode proved that laccase maintained its good biological activity and played an essential role in catalyzing GA.

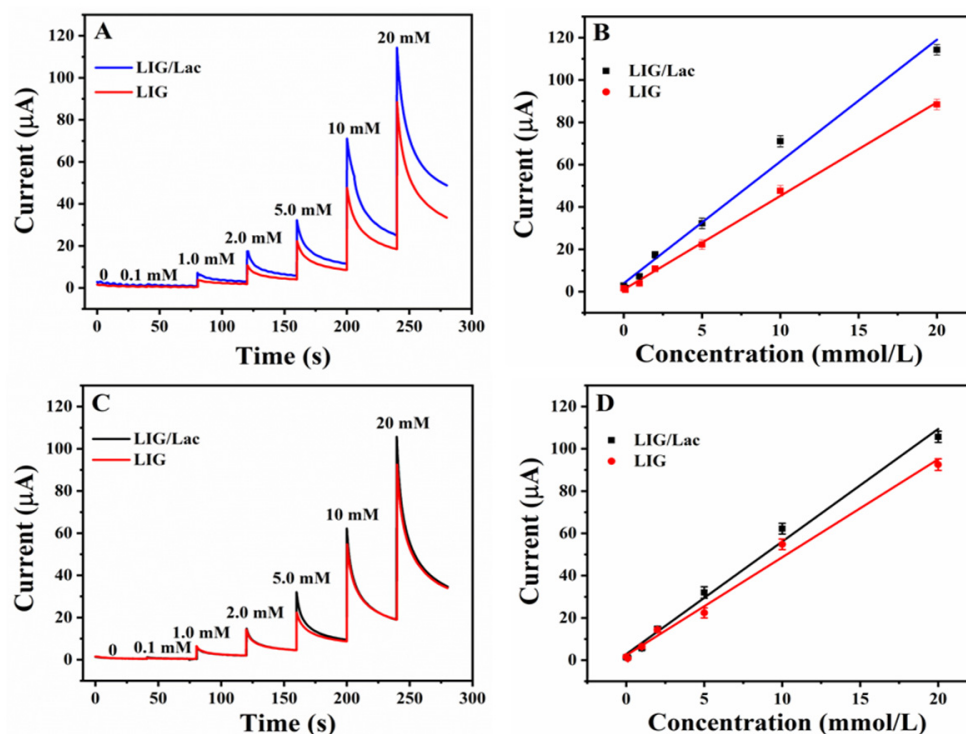


**Figure 4.** The Chronoamperometric records of LIG and LIG/Lac electrodes after the addition of increasing amounts of GA (A,C) and corresponding calibration plot (B,D). Applied potential is 0.4 V vs. Ag/AgCl (A,B) and 0.5 V (C,D). Number of repetitions is  $n = 3$ . 10 mmol/L PBS at pH 4.0. The order of GA adding concentration: 0, 0.1, 1.0, 2.0, 5.0, 10, 20 mmol/L.

In addition, considering that the current signals showed significant differences between the LIG and LIG/Lac electrodes when the applied potential was at 0.5 V, the constant voltage of 0.4 V was selected for chronoamperometry analysis. In addition, the linear relationship of LIG and LIG/Lac electrodes for GA analysis in the range of 0.1–20 mmol/L were shown in Table 1. The large slope of the linear regression line at 0.4 V for the LIG/Lac electrode reflected its good sensitivity for GA analysis. The detection limit is 0.07 mmol/L, which is comparable to that of other electrochemical sensors. From Figure 2D, it can be seen that the modification of laccase hinders electron transfer on the electrode surface. However, from Table 1, it can be seen that the modification of laccase improves the sensitivity of GA detection. Although the slope increase is not significant compared to the LIG electrode, this is due to the oriented catalysis of laccase. LIG has a certain response to substances with oxidation–reduction properties, which belong to non-specific reactions. Therefore, selectivity and actual sample analysis are key indicators for evaluating sensor performance.

**Table 1.** The linear relationship of LIG and LIG/Lac electrodes for GA analysis.

Electrodes	Potential (V)	Linear Equation	Linear Range mmol/L	Coefficient of Determination ( $R^2$ )
LIG	0.4	$y = 4.42x + 1.01$	0.1–20	0.9982
LIG/Lac		$y = 5.75x + 3.94$		0.9877
LIG	0.5	$y = 4.64x + 2.31$		0.9906
LIG/Lac		$y = 5.33x + 2.85$		

### 3.5. Interferences Study and Matrix Effect

To investigate the selectivity of the prepared GA sensor, the effect of the common coexistence of species, such as glucose, galactose, lactobionic acid, and arginine, were selected as the interferences to assess the selectivity of the prepared biosensor towards

GA. As shown in Figure 5A, there were no significant current responses to the potential interfering substances in the presence of GA, which indicated that the LIG/Lac electrode exhibited high selectivity towards GA.

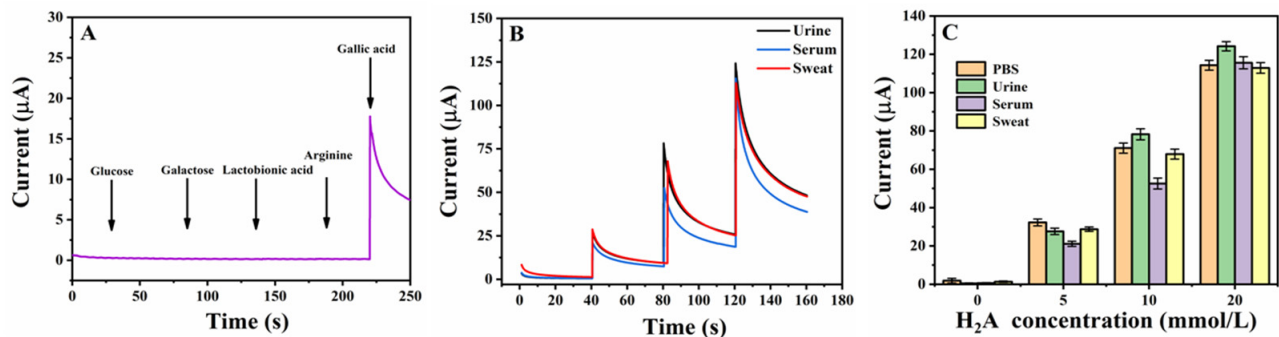


**Figure 5.** (A) Interferent study of the LIG/Lac electrode after addition of 5.0 mmol/L glucose, galactose, lactobionic acid, arginine, and GA in turn. Applied potential is 0.4 V vs. Ag/AgCl; Measurement volume 50 µL 0.1 mol/L PBS at pH 4.0, adding volume 10 µL. (B) *i*-*t* curves, and (C) matrix effect for GA determination using LIG/Lac electrode in body fluid samples. Applied potential 0.4 V, *n* = 3. Measurement volume: 50 µL; Real samples were diluted 1:2 with 0.1 M PBS pH 4.0.

In addition, considering that the present laccase-based biosensors might suffer from interferents in fluid body samples, potentially actual samples such as urine, serum, and sweat were investigated to evaluate the effect of the sample matrixes on the analytical results. Using the method of standard additions, high, medium, and low concentrations of GA were gradually added to the artificial urine, FBS, and artificial sweat solutions which were 1:1 diluted by 0.1 mol/L PBS (pH 4.0). As shown in Figure 5B, the current responses among the three matrixes were significantly lower. With the increase in GA added concentration, the current responses increased accordingly. Good current signals were generated by high, medium, and low concentrations of GA in the urine, serum, and sweat solutions indicating that the performance of the GA sensor was not significantly affected by the sample matrix (Figure 5C). Recovery rates were determined by spiking three types of body fluids with 5, 10, and 20 mmol/L. Table 2 displays the GA recoveries in body fluids. Results showed that the recoveries ranged from 69.85% to 114.05%, with coefficients of variation from 2.5 to 7.1%. All the above results indicated that the constructed GA sensor was a feasible method for analyzing GA in real samples without significant matrix interference.

**Table 2.** Analysis of GA recoveries in body fluids.

Samples	Added Concentration (mmol/L)	Found Current (µA)	Recoveries (%)
Urine	0	0.49	-
	5	27.59	92.18
	10	78.27	114.05
	20	124.2	111.01
Serum	0	0.59	-
	5	21.12	69.85
	10	52.56	76.21
	20	115.6	103.21
Sweat	0	1.35	-
	5	28.75	93.20
	10	67.93	97.62
	20	112.9	100.10

Table 2. Cont.

Samples	Added Concentration (mmol/L)	Found Current ( $\mu\text{A}$ )	Recoveries (%)
PBS	0	2.86	-
	5	32.26	-
	10	71.06	-
	20	114.29	-

### 3.6. Regeneration and Storage Stability Studies

Regeneration is an essential property for the application of the GA sensor. After GA determination, the sensor regeneration was carried out by reusing the eluted LIG/Lac electrode. As reported in Figure 6A, the current change toward GA sensing was reduced slightly, possibly due to the gradual inactivation of laccase during repeated electrochemical determination. Nevertheless, good current responses were still retained after nine times of regeneration. Nearly 90% of the laccase activity was retained after five consecutive measurements, and the current signal decreased slightly to about 80% and 70% after seven and nine measurements, respectively. The long-term storage stability of the LIG/Lac electrode for the GA sensor was also evaluated by measuring the current response to 5 mmol/L GA for eight days under sealed storage at 4 °C. As shown in Figure 6B, the GA sensor retained about 82% of its initial response after eight days of storage. The excellent regeneration and long-term stability highlight the extensive application prospect of the prepared GA sensor.

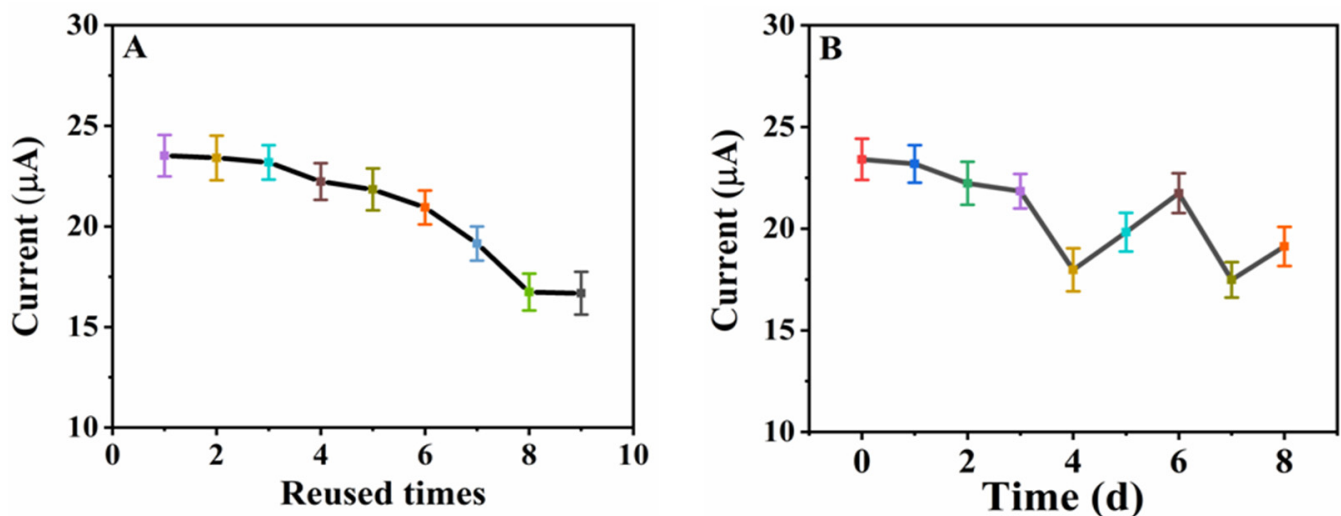


Figure 6. Reproducibility (A) and stability (B) of the LIG/Lac electrode for GA sensing. Applied potential 0.4 V vs. Ag/AgCl,  $n = 3$ . 0.1 M PBS pH 4.0. GA concentration: 5.0 mmol/L.

Table 3 compares the performance characteristics of different GA electrochemical sensors. As can be seen in Table 3, the modification process for most methods is complex and tends to be more time-consuming and costly. Compared with other methods, our work shows a series of advantages, such as simple and convenient operation, low cost, excellent selectivity, good stability, and regeneration, indicating its some potential applications in GA assays.

**Table 3.** The comparison of electrochemical sensors for determination of GA.

Ref.	Electrode	Modified Materials	Determination Method	Linear Range	Detection Limit	Merits	Shortcoming
[22]	Screen printed carbon electrode	No	DPV *	0.1–2.0 mmol/L	0.049 mmol/L (Depending on pH)	Real samples: wine, green tea, apple juice and serum fortified with GA; Low response time; Established conditions of pH; Convenient operation	No stability and regeneration tests
[15]	Paraffin wax impregnated graphite electrode	Thionine + nickel hexacyanoferrate	DPV	$4.99 \times 10^{-6}$ – $1.20 \times 10^{-3}$ mol/L	$4.99 \times 10^{-6}$ mmol/L	Good stability and reproducibility; Excellent sensitivity; Tea sample analysis	Complex electrode modification process
[39]	Glassy carbon electrode	Graphene oxide nanocolloids and SiO <sub>2</sub> -nanoparticles	DPV	$6.25 \times 10^{-6}$ – $1.0 \times 10^{-3}$ mmol/L	$2.09 \times 10^{-6}$ mol/L	Good stability and reproducibility; Excellent sensitivity; Analyzing red wine, white wine and orange juice,	Complex material preparation
[40]	Glassy carbon electrode	zirconium fumarate metal-organic framework and mesoporous carbon composite	DPV	0.2–5 and 5–100 $\mu$ mol/L	0.15 $\mu$ mol/L	Comparable sensitivity and selectivity; Wider linear range; Satisfactory reproducibility and Long -term stability; green tea sample analysis	Complex material preparation
This work	LIG electrode	Lac	Chronoam-perometry	0.1–20 mmol/L	0.07 mmol/L	Flexibility; Simple and convenient operation; Low cost; Good stability and regeneration; Excellent selectivity; Analyzing complex biological samples	Competitive sensitivity

\* DPV: Differential Pulse Voltammetry.

#### 4. Conclusions

This work presented a simple, rapid, and easy electrochemical sensor for GA determination based on LIG/lac electrodes. The integrated LIG electrode with a classical three-electrode system was successfully fabricated by one-step direct laser writing over a PI film. Surface modification of LIG-based electrodes with laccase through covalent crosslinking of glutaraldehyde provides a bio-recognition element for high selectivity of GA determination. Under the optimum conditions, the LIG/lac sensor showed excellent catalytic activity toward GA and exhibited a linear GA determination range from 0.1 to 20 mmol/L with high sensitivity. Additionally, the biosensor displayed high specificity for GA, both in pure and coexistence of the common interfering species, and effectively discriminated interferents in potentially actual samples (e.g., urine, serum, sweat). The method's applicability was also demonstrated by studying regeneration and storage stability. The results show that the biosensor had a good regeneration performance after seven measurements and long-term storage stability within eight days. Overall, the constructed electrochemical sensor offers a simple, portable, economical, specific, and accurate tool for GA determination in complex biological samples.

**Author Contributions:** Y.L. and X.L. designed the experiments. Y.Z., Z.L., R.C. and W.C. performed the experiments. X.L. and Y.Z. analyzed the data. Y.L. guided the study and wrote the manuscript. X.M. organized and revised the manuscript. X.L. and X.M. provided fund support. All authors have read and agreed to the published version of the manuscript.

**Funding:** This project was financially supported by Fujian Province Natural Science Foundation (2020J01835), the National Innovation and Entrepreneurship Program for College Students (20221039016), the Natural Science Foundation of Shandong Province (ZR2021MH146), and the Medicine and Health Science and Technology Development Plan Project of Shandong Province (202012060616).

**Institutional Review Board Statement:** Not applicable.

**Informed Consent Statement:** Not applicable.

**Data Availability Statement:** Data are contained within the article.

**Conflicts of Interest:** The authors declare no conflict of interest.

#### References

1. Ranga, R.; Kumar, A.; Kumari, P.; Singh, P.; Madaan, V.; Kumar, K. Ferrite application as an electrochemical sensor: A review. *Mater. Charact.* **2021**, *178*, 111269. [[CrossRef](#)]
2. Teymourian, H.; Parrilla, M.; Sempionatto, J.R.; Montiel, N.F.; Barfidokht, A.; Van Echelpoel, R.; De Wael, K.; Wang, J. Wearable Electrochemical Sensors for the Monitoring and Screening of Drugs. *ACS Sens.* **2020**, *5*, 2679–2700. [[CrossRef](#)] [[PubMed](#)]
3. Yola, M.L.; Atar, N.; Ozcan, N. A novel electrochemical lung cancer biomarker cytokeratin 19 fragment antigen 21-1 immunosensor based on Si<sub>3</sub>N<sub>4</sub>/MoS<sub>2</sub> incorporated MWCNTs and core-shell type magnetic nanoparticles. *Nanoscale* **2021**, *13*, 4660–4669. [[CrossRef](#)]
4. Forouzanfar, S.; Alam, F.; Pala, N.; Wang, C. Highly sensitive label-free electrochemical aptasensors based on photoresist derived carbon for cancer biomarker detection. *Biosens. Bioelectron.* **2020**, *170*, 112598. [[CrossRef](#)]
5. Dong, W.; Niu, X.; Ji, X.; Chen, Y.; Kong, L.B.; Kang, L.; Ran, F. Transferring Electrochemically Active Nanomaterials into a Flexible Membrane Electrode via Slow Phase Separation Method Induced by Water Vapor. *ACS Sustain. Chem. Eng.* **2019**, *7*, 4295–4306. [[CrossRef](#)]
6. Huang, S.; Zhang, L.; Dai, L.; Wang, Y.; Tian, Y. Nonenzymatic Electrochemical Sensor with Ratiometric Signal Output for Selective Determination of Superoxide Anion in Rat Brain. *Anal. Chem.* **2021**, *93*, 5570–5576. [[CrossRef](#)]
7. Wang, M.; Zhang, X. Femtosecond Thin-Film Laser Amplifiers Using Chirped Gratings. *ACS Omega* **2019**, *4*, 7980–7986. [[CrossRef](#)]
8. Trusovas, R.; Niaura, G.; Gaidukevic, J.; Malisauskaitė, I.; Barkauskas, J. Graphene oxide-dye nanocomposites: Effect of molecular structure on the quality of laser-induced graphene. *Nanotechnology* **2018**, *29*, 445704. [[CrossRef](#)]
9. Wang, H.; Zhao, Z.; Liu, P.; Guo, X. Laser-Induced Graphene Based Flexible Electronic Devices. *Biosensors* **2022**, *12*, 55. [[CrossRef](#)]
10. Liao, J.; Zhang, X.; Sun, Z.; Chen, H.; Fu, J.; Si, H.; Ge, C.; Lin, S. Laser-Induced Graphene-Based Wearable Epidermal Ion-Selective Sensors for Noninvasive Multiplexed Sweat Analysis. *Biosensors* **2022**, *12*, 397. [[CrossRef](#)]
11. Wan, Z.; Nguyen, N.T.; Gao, Y.; Li, Q. Laser induced graphene for biosensors. *Sustain. Mater. Technol.* **2020**, *25*, e00205. [[CrossRef](#)]
12. Fenzl, C.; Nayak, P.; Hirsch, T.; Wolfbeis, O.S.; Alshareef, H.N.; Baeumner, A.J. Laser-Scribed Graphene Electrodes for Aptamer-Based Biosensing. *ACS Sens.* **2017**, *2*, 616–620. [[CrossRef](#)] [[PubMed](#)]

13. Santos, N.F.; Pereira, S.O.; Moreira, A.; Girão, A.V.; Carvalho, A.F.; Fernandes, A.J.S.; Costa, F.M. IR and UV Laser-Induced Graphene: Application as Dopamine Electrochemical Sensors. *Adv. Mater. Technol.* **2021**, *6*, 202100007. [[CrossRef](#)]
14. Oliveira, M.E.; Lopes, B.V.; Rossato, J.H.H.; Maron, G.K.; Gallo, B.B.; Rosa, A.; Borges, L.R.; Balboni, D.C.; Alves, M.L.F.; Ferreira, M.R.A.; et al. Electrochemical Biosensor Based on Laser-Induced Graphene for COVID-19 Diagnosing: Rapid and Low-Cost Detection of SARS-CoV-2 Biomarker Antibodies. *Surfaces* **2022**, *5*, 187–201. [[CrossRef](#)]
15. Sangeetha, N.S.; Narayanan, S.S. A novel bimediator amperometric sensor for electrocatalytic oxidation of gallic acid and reduction of hydrogen peroxide. *Anal. Chim. Acta* **2014**, *828*, 34–45. [[CrossRef](#)] [[PubMed](#)]
16. Fernandes, F.H.; Salgado, H.R. Gallic Acid: Review of the Methods of Determination and Quantification. *Crit. Rev. Anal. Chem.* **2016**, *46*, 257–265. [[CrossRef](#)]
17. Chen, L.; Yang, J.; Chen, W.; Sun, S.; Tang, H.; Li, Y. Perovskite mesoporous LaFeO<sub>3</sub> with peroxidase-like activity for colorimetric detection of gallic acid. *Sens. Actuators B Chem.* **2020**, *321*, 128642. [[CrossRef](#)]
18. Saeed, S.; Bibi, I.; Mehmood, T.; Naseer, R.; Bilal, M. Valorization of locally available waste plant leaves for production of tannase and gallic acid by solid-state fermentation. *Biomass Convers. Biorefin.* **2020**, *12*, 3809–3816. [[CrossRef](#)]
19. Li, S.; Sun, H.; Wang, D.; Qian, L.; Zhu, Y.; Tao, S. Determination of Gallic Acid by Flow Injection Analysis Based on Luminol-AgNO<sub>3</sub>-Ag NPs Chemiluminescence System. *Chin. J. Chem.* **2012**, *30*, 837–841. [[CrossRef](#)]
20. Alam, P.; Kamal, Y.T.; Alqasoumi, S.I.; Foudah, A.I.; Alqarni, M.H.; Yusufoglu, H.S. HPTLC method for simultaneous determination of ascorbic acid and gallic acid biomarker from freeze dry pomegranate juice and herbal formulation. *Saudi Pharm. J.* **2019**, *27*, 975–980. [[CrossRef](#)]
21. Yang, T.; Zhang, Q.; Chen, T.; Wu, W.; Tang, X.; Wang, G.; Feng, J.; Zhang, W. Facile potentiometric sensing of gallic acid in edible plants based on molecularly imprinted polymer. *J. Food Sci.* **2020**, *85*, 2622–2628. [[CrossRef](#)] [[PubMed](#)]
22. Badea, M.; di Modugno, F.; Floroian, L.; Tit, D.M.; Restani, P.; Bungau, S.; Iovan, C.; Badea, G.E.; Aleya, L. Electrochemical strategies for gallic acid detection: Potential for application in clinical, food or environmental analyses. *Sci. Total Environ.* **2019**, *672*, 129–140. [[CrossRef](#)] [[PubMed](#)]
23. Monteiro, M.C.; Winiarski, J.P.; Santana, E.R.; Szpoganicz, B.; Vieira, I.C. Ratiometric Electrochemical Sensor for Butralin Determination Using a Quinazoline-Engineered Prussian Blue Analogue. *Materials* **2023**, *16*, 1024. [[CrossRef](#)] [[PubMed](#)]
24. Li, S.Y.; Hong, D.; Chen, W.J.; Wang, J.; Sun, K. Extracellular laccase-activated humification of phenolic pollutants and its application in plant growth. *Sci. Total Environ.* **2022**, *802*, 150005. [[CrossRef](#)]
25. Arica, M.Y.; Salih, B.; Celikbicak, O.; Bayramoglu, G. Immobilization of laccase on the fibrous polymer-grafted film and study of textile dye degradation by MALDI-TOF-MS. *Chem. Eng. Res. Des.* **2017**, *128*, 107–119. [[CrossRef](#)]
26. Lonappan, L.; Rouissi, T.; Laadila, M.A.; Brar, S.K.; Galan, L.H.; Verma, M.; Surampalli, R.Y. Agro-industrial-Produced Laccase for Degradation of Diclofenac and Identification of Transformation Products. *ACS Sustain. Chem. Eng.* **2017**, *5*, 5772–5781. [[CrossRef](#)]
27. Castrovilli, M.C.; Tempesta, E.; Cartoni, A.; Plescia, P.; Bolognesi, P.; Chiarinelli, J.; Calandra, P.; Cicco, N.; Verrastro, M.F.; Centonze, D.; et al. Fabrication of a New, Low-Cost, and Environment-Friendly Laccase-Based Biosensor by Electro spray Immobilization with Unprecedented Reuse and Storage Performances. *ACS Sustain. Chem. Eng.* **2022**, *10*, 1888–1898. [[CrossRef](#)]
28. Agrawal, K.; Verma, P. Laccase: Addressing the ambivalence associated with the calculation of enzyme activity. *3 Biotech* **2019**, *9*, 365. [[CrossRef](#)]
29. Wasak, A.; Drozd, R.; Jankowiak, D.; Rakoczy, R. Rotating magnetic field as tool for enhancing enzymes properties—Laccase case study. *Sci. Rep.* **2019**, *9*, 3707. [[CrossRef](#)]
30. Nazari, M.; Kashanian, S.; Rafipour, R. Laccase immobilization on the electrode surface to design a biosensor for the detection of phenolic compound such as catechol. *Spectrochim. Acta Part A Mol. Biomol. Spectrosc.* **2015**, *145*, 130–138. [[CrossRef](#)]
31. Demkiv, O.; Gayda, G.; Stasyuk, N.; Brahinetz, O.; Gonchar, M.; Nisnevitch, M. Nanomaterials as Redox Mediators in Laccase-Based Amperometric Biosensors for Catechol Assay. *Biosensors* **2022**, *12*, 741. [[CrossRef](#)] [[PubMed](#)]
32. Pimpilova, M.; Kamarska, K.; Dimcheva, N. Biosensing Dopamine and L-Epinephrine with Laccase (*Trametes pubescens*) Immobilized on a Gold Modified Electrode. *Biosensors* **2022**, *12*, 719. [[CrossRef](#)] [[PubMed](#)]
33. Wang, G.Y.; Chen, J.Y.; Huang, L.; Chen, Y.T.; Li, Y.X. A laser-induced graphene electrochemical immunosensor for label-free CEA monitoring in serum. *Analyst* **2021**, *146*, 6631–6642. [[CrossRef](#)] [[PubMed](#)]
34. Winiarski, J.P.; de Melo, D.J.; Santana, E.R.; Santos, C.S.; de Jesus, C.G.; Fujiwara, S.T.; Wohnrath, K.; Pessôa, C.A. Layer-by-Layer Films of Silsesquioxane and Nickel(II) Tetrasulphophthalocyanine as Glucose Oxidase Platform Immobilization: Amperometric Determination of Glucose in Kombucha Beverages. *Chemosensors* **2023**, *11*, 346. [[CrossRef](#)]
35. Wan, Z.; Umer, M.; Lobino, M.; Thiel, D.; Nguyen, N.T.; Trinchi, A.; Shiddiky, M.J.A.; Gao, Y.; Li, Q. Laser induced self-N-doped porous graphene as an electrochemical biosensor for femtomolar miRNA detection. *Carbon* **2020**, *163*, 385–394. [[CrossRef](#)]
36. Joanni, E.; Kumar, R.; Fernandes, W.P.; Savu, R.; Matsuda, A. In situ growth of laser-induced graphene micro-patterns on arbitrary substrates. *Nanoscale* **2022**, *14*, 8914–8918. [[CrossRef](#)]
37. Settu, K.; Lai, Y.C.; Liao, C.T. Carbon nanotube modified laser-induced graphene electrode for hydrogen peroxide sensing. *Mater. Lett.* **2021**, *300*, 130106. [[CrossRef](#)]
38. Zhang, Z.; Song, M.; Hao, J.; Wu, K.; Li, C.; Hu, C. Visible light laser-induced graphene from phenolic resin: A new approach for directly writing graphene-based electrochemical devices on various substrates. *Carbon* **2018**, *127*, 287–296. [[CrossRef](#)]

39. Chikere, C.O.; Faisal, N.H.; Kong Thoo Lin, P.; Fernandez, C. The synergistic effect between graphene oxide nanocolloids and silicon dioxide nanoparticles for gallic acid sensing. *J. Solid. State Electr.* **2019**, *23*, 1795–1809. [[CrossRef](#)]
40. Liu, H.; Hassan, M.; Bo, X.; Guo, L. Fumarate-based metal-organic framework/mesoporous carbon as a novel electrochemical sensor for the detection of gallic acid and luteolin. *J. Electroanal. Chem.* **2019**, *849*, 113378. [[CrossRef](#)]

**Disclaimer/Publisher's Note:** The statements, opinions and data contained in all publications are solely those of the individual author(s) and contributor(s) and not of MDPI and/or the editor(s). MDPI and/or the editor(s) disclaim responsibility for any injury to people or property resulting from any ideas, methods, instructions or products referred to in the content.